

Article

Cloning and Molecular Characterization of the *phlD* Gene Involved in the Biosynthesis of “Phloroglucinol”, a Compound with Antibiotic Properties from Plant Growth Promoting Bacteria *Pseudomonas* spp.

Payal Gupta ^{1,†}, Prasanta K. Dash ^{1,*,†}, Tenkabailu Dharmanna Sanjay ¹, Sharat Kumar Pradhan ^{2,3} , Rohini Sreevathsa ¹  and Rhitu Rai ^{1,*}

¹ ICAR-National Institute for Plant Biotechnology, Pusa Campus, New Delhi 110012, India

² ICAR-National Rice Research Institute, Cuttack 753006, India

³ Indian Council of Agriculture Research, Krishi Bhawan, New Delhi 110001, India

* Correspondence: prasanta01@yahoo.com (P.K.D.); rhitunrcpb@yahoo.com (R.R.); Tel.: +91-1125841787 (P.K.D.); Fax: +91-1125843984 (P.K.D.)

† These authors contributed equally to this work and share first authorship.

Abstract: *phlD* is a novel kind of polyketide synthase involved in the biosynthesis of non-volatile metabolite phloroglucinol by iteratively condensing and cyclizing three molecules of malonyl-CoA as substrate. Phloroglucinol or 2,4-diacetylphloroglucinol (DAPG) is an ecologically important rhizospheric antibiotic produced by pseudomonads; it exhibits broad spectrum anti-bacterial and anti-fungal properties, leading to disease suppression in the rhizosphere. Additionally, DAPG triggers systemic resistance in plants, stimulates root exudation, as well as induces phyto-enhancing activities in other rhizobacteria. Here, we report the cloning and analysis of the *phlD* gene from soil-borne gram-negative bacteria—*Pseudomonas*. The full-length *phlD* gene (from 1078 nucleotides) was successfully cloned and the structural details of the PHLD protein were analyzed in-depth via a three-dimensional topology and a refined three-dimensional model for the PHLD protein was predicted. Additionally, the stereochemical properties of the PHLD protein were analyzed by the Ramachandran plot, based on which, 94.3% of residues fell in the favored region and 5.7% in the allowed region. The generated model was validated by secondary structure prediction using PDBsum. The present study aimed to clone and characterize the DAPG-producing *phlD* gene to be deployed in the development of broad-spectrum biopesticides for the biocontrol of rhizospheric pathogens.

Keywords: phloroglucinol; polyketide; DAPG; *phlD*; Ramachandran plot; PMDB



Citation: Gupta, P.; Dash, P.K.; Sanjay, T.D.; Pradhan, S.K.; Sreevathsa, R.; Rai, R. Cloning and Molecular Characterization of the *phlD* Gene Involved in the Biosynthesis of “Phloroglucinol”, a Compound with Antibiotic Properties from Plant Growth Promoting Bacteria *Pseudomonas* spp. *Antibiotics* **2023**, *12*, 260. <https://doi.org/10.3390/antibiotics12020260>

Academic Editors: Theodoros Karampatakis and Grzegorz Wegrzyn

Received: 30 October 2022

Revised: 21 December 2022

Accepted: 23 December 2022

Published: 28 January 2023



Copyright: © 2023 by the authors. Licensee MDPI, Basel, Switzerland. This article is an open access article distributed under the terms and conditions of the Creative Commons Attribution (CC BY) license (<https://creativecommons.org/licenses/by/4.0/>).

1. Introduction

Plant growth-promoting rhizobacteria (PGPR) are bacteria that colonize some or all parts of the rhizosphere environment and have the capability to promote plant growth [1–3] either directly by antibiosis or indirectly by quorum sensing. PGPR produce non-volatile metabolites that can directly stimulate plant growth, inhibit plant pathogens, and/or induce host–defense mechanisms against pathogens [4,5]. *Pseudomonas fluorescens* is an important group of PGPR that suppress root and seedling diseases by producing non-volatile secondary metabolite phloroglucinol. Genetic methods [6–8] and direct isolation from the soils of diseased plants [9–11] have shown the importance of DAPG and its derivatives as biocontrol activity agents. These compounds act as antibiotics, antimicrobials or antifungals, signaling molecules, and pathogenicity factors. Several antibacterial and antifungal compounds from plants have been characterized [12] and their mechanisms of action have been delineated [13]; biosynthesis and genetic regulation of DAPG in the *Pseudomonas* spp. have been the focus of active research.

Most of the genes required for the biosynthesis of DAPG have been cloned and characterized from different strains of *Pseudomonas*. These genes are recognized as conserved in 2,4-DAPG, producing pseudomonads that have been isolated from various soil samples collected from around the world [14–16]. All of the genes are arranged as an operon on the *phl* locus, spanning a genomic fragment of ~6.5 kb, comprising six genes, viz. *phlA*, *phlB*, *phlC*, *phlD*, *phlE*, and *phlF*. While *phlA*, *phlB*, *phlC*, and *phlD* are transcribed as an operon; they are flanked on either side by *phlE* and *phlF*. *phlE* codes for an efflux protein and *phlF* encodes a repressor protein (Figure 1).

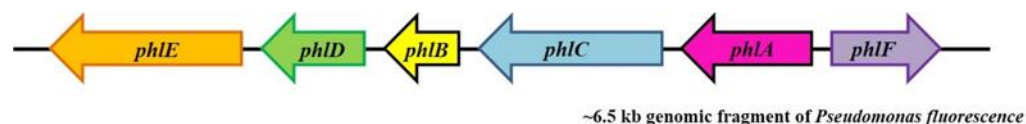


Figure 1. Schematic representation of a ~6.5 kb genomic fragment of *Pseudomonas* harboring the genes responsible for the biosynthesis of 2,4-DAPG by *phl* operon. *phl* operon comprises four genes *phlA*, *phlB*, *phlC*, and *phlD*. The operon is flanked on either side by *phlE* and *phlF* genes that are separately transcribed and coded for the putative efflux and regulatory (repressor) proteins, respectively. They are not required for phloroglucinol production.

The DAPG gene cluster is self-sufficient for the biosynthesis and regulation of 2,4-diacetylphloroglucinol. Amongst all genes, *phlD* is the key gene responsible for the production of (MAPG), while, *phlA*, *phlB*, and *phlC* are necessary to convert MAPG to 2,4-DAPG. Products of these genes resemble neither type I nor type II PKS enzyme systems. Rather, *PhlD* shows similarity to plant chalcone synthases, indicating that phloroglucinol synthesis is mediated by a novel kind of PKS [17–19].

Apart from changes in gene expression, the production of 2,4-DAPG in many strains of fluorescent *Pseudomonas* spp. is stimulated by physical factors, such as a concentration of glucose [20] or concentrations of sucrose/ethanol [19,21]. Moreover, zinc sulfate and ammonium molybdate have been reported to favor 2,4-DAPG production in some strains, whereas inorganic phosphate in general has an inhibitory effect [20].

phlD gene, responsible for the bio-synthesis of MAPG, shows similarity to novel type III polyketide synthase (PKS) [22]. *phlD* iteratively condenses three molecules of malonyl-CoA that subsequently cyclize [23] to form mono-acetyl phloroglucinol (MAPG). However, it is delineated that *PhlD* catalyzes the condensation of three molecules of malonyl-CoA into 3,5-diketoheptanedioate [24] and this polyketide intermediate through decarboxylation/cyclization, forms phloroglucinol [25].

Our laboratory has isolated and cloned and characterized *phlA*, *phlB*, and *phlC*; the downstream genes [26–28] of *phl* operon, and the current study focuses on the cloning and characterization of the *phlD* gene, an upstream/first committed step of the *phl* operon of *Pseudomonas* and its in-depth characterization to obtain deep insight into the *PHLD* function. This will help in fine-tuning (upregulating/downregulating) the bio-synthesis of 2,4-DAPG in response to potent fungal and bacterial pathogens for improving the biocontrols of plant pathogens.

2. Materials and Methods

2.1. Genomic DNA Isolation and PCR Amplification of the *phlD* Gene

Genomic DNA of the *Pseudomonas* spp. strain RS9 (KP057506) [29] was isolated as described earlier [26]. The *phlD* gene from *Pseudomonas* spp. was amplified by the polymerase chain reaction-based strategy. The forward and reverse primers were designed using the PRIMER 3 tool, viz, *phlD* (FP): CCGACTAGTAGGACTTGTCATGTCTACTCTTTG and *phlD* (RP): GGAAAGCTTCGTGCAATGTGTTGGTCTGTCA were designed using the nucleotide sequence of *Pseudomonas fluorescens* (U41818) available in the EMBL database. Restriction sites for the enzymes *SpeI* and *HindIII* were incorporated at the 5' ends of forward and reverse primers (underlined sequences), respectively. The PCR reaction mixture

consisted of 10 pmol of each primer, 50 ng of template DNA, 50 mM KCl, 10 mM Tris-HCl (pH 9.0), 0.1% Triton, 2.5 mM MgCl₂, 0.2 mM of each dNTP, and a 1.25 unit of Phusion *Taq* DNA polymerase in 100 µL of volume. The thermal cycling was performed with an initial denaturation cycle of 3 min at 98 °C, followed by 30 cycles of (i) denaturation at 98 °C for 20 s; (ii) annealing for 30 s at 55 °C; (iii) extension for 30 s at 72 °C, as well as one cycle of the final extension for 7 min at 72 °C.

2.2. Cloning of the *phlD* Gene in pBluescript (SK+) Vector

For cloning of the PCR amplified *phlD* gene into the pBluescript (SK+) vector, the PCR product (insert) and pBluescript (SK+) vector DNA were double digested with *SpeI* and *HindIII*. The reaction mixture was incubated at 37 °C for 3 hours. Restricted DNA was gel-purified using a Zymo clean gel DNA recovery kit. Purified 50 ng of linearized pBluescript vector and 100 ng of a double-digested PCR product were ligated using T₄ DNA ligase. The ligated mixture was incubated at 4 °C overnight for ligation and used for transformation into *E. coli*. The transformed colonies (white in color) obtained after overnight incubation at 37 °C were picked and streaked onto fresh LA-carbenicillin (100 µg/mL) plates.

2.3. Confirmation of Cloning and Sequencing

Recombinant colonies were confirmed by restriction digestion with *SpeI*+*HindIII* enzymes. The restricted DNA samples were analyzed on 1.2% agarose gel. The complete nucleotide sequence was determined by the Sanger di-deoxy sequencing. M13F and M13R primers were used for sequencing. *phlD* gene-specific primers were also used for confirming the sequence. The final sequence was determined from both strands and a comparison of *phlD* nucleic acid and amino acid sequences with already existing sequences was performed. The deduced amino acid sequence of PHLD from *Pseudomonas* RS-9 was compared with type III PKS from gram-positive bacteria and other plants by a multiple sequence alignment using MAFFT version 7.271 program [30] with the L-INS-I strategy and output in Phylip format. A similarity score for each nucleotide of the aligned sequences was calculated by ESPRIPT 3.0 [31] (<https://espript.ibcp.fr/ESPrIPT/ESPrIPT/>, accessed on 20 February 2022) with default parameters. Conserved domain annotation analysis was performed using InterProScan [32].

2.4. Phylogenetic Analysis

For estimation of the phylogenetic relationship between PHLD from various *Pseudomonas* strains and type III PKS from gram-positive bacteria and plants, the amino acid sequences were retrieved from the NCBI database. A multiple sequence alignment for the respective amino acid sequences was performed by Clustal Omega [33] and an un-rooted tree was constructed in MEGA10 [34] using the maximum likelihood (ML) method. Tree topology was searched using the nearest neighbor interchanges (NNIs) algorithm [35]. The LG+G+I substitution model was employed. The gamma shape parameter was estimated directly from the data and the analysis was performed using 1000 bootstrap replicates. The proportion of invariable sites was fixed. The tree was obtained in the Newick format.

2.5. Structure Prediction

The model of the PHLD protein was predicted using the I-TASSER server (<http://zhanglab.ccmb.med.umich.edu/I-TASSER/>, accessed on 25 February 2022) [36]. I-TASSER (Iterative Threading ASSEMBly Refinement) is a hierarchical approach to protein structures and function prediction. Structural templates were first identified from PDB by the multiple threading approach, LOMETS; full-length atomic models were then constructed by iterative template fragment assembly simulations. The generated model was refined using ModRefiner (<http://zhanglab.ccmb.med.umich.edu/ModRefiner/>, accessed on 3 March 2022). ModRefiner is an algorithm for high-resolution protein structure refinement. Both side-chain and backbone atoms were completely flexible during structure refinement simulations. ModRefiner allowed the assignment of a second structure that was

used as a reference to which the refinement simulations were driven. The ModRefiner was used to draw the initial starting model of PHLD closer to its native state.

2.6. Ramachandran Plot Analysis

The stereochemical properties of the PHLD protein were assessed by the Ramachandran plot analysis using RAMPAGE [37]. This allowed visualization of energetically allowed regions for backbone dihedral angles ψ against ϕ of amino acid residues in the PHLD protein structure. The residues in the disallowed region were further refined by using Modloop (<https://modbase.compbio.ucsf.edu/modloop/>, accessed on 5 March 2022). Modloop relies on MODELLER, which predicts the loop conformations of PHLD by the satisfaction of spatial restraints, without relying on a database of known protein structures [38].

2.7. Validation and Visualization of Modeled Structure

The validation of the modeled structure was performed using PDBsum [39] and PROCHECK [40]. Structure visualization was performed using PyMOL. The predicted model of the protein was submitted to the Protein Model Database [41] (<http://srv00.recas.ba.infn.it/PMDB/main.php>, accessed on 10 March 2022).

3. Results

PCR amplification of the *phlD* gene from the genomic DNA of the *Pseudomonas* spp. strain RS9 (KP057506) [29] resulted in a fragment of 1 kb (Figure 2). The amplified PCR product and pBluescript control vector were then restricted with *SpeI* and *HindIII* restriction enzymes. This resulted in a 1 kb fragment PCR product with sticky ends (insert) and 3 kb of linearized control vector pBluescript (SK+) with sticky ends for *SpeI* and *HindIII* (Figure 3). The purified double-digested PCR product (insert) was ligated into the linearized pBluescript vector.

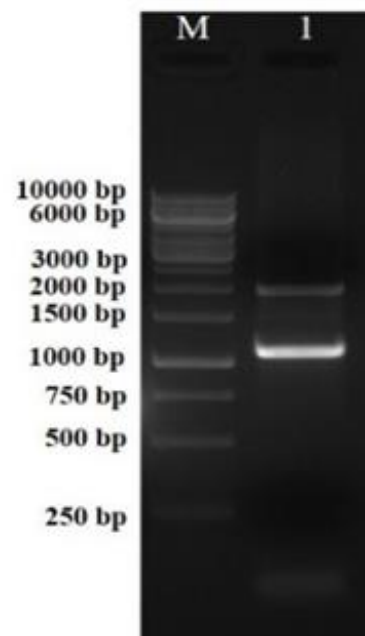


Figure 2. PCR amplification of the *phlD* gene from genomic DNA of *Pseudomonas fluorescens*. Lane M: 1 kb DNA ladder; Lane 1: ~1078 kb amplicon of the *phlD* gene.

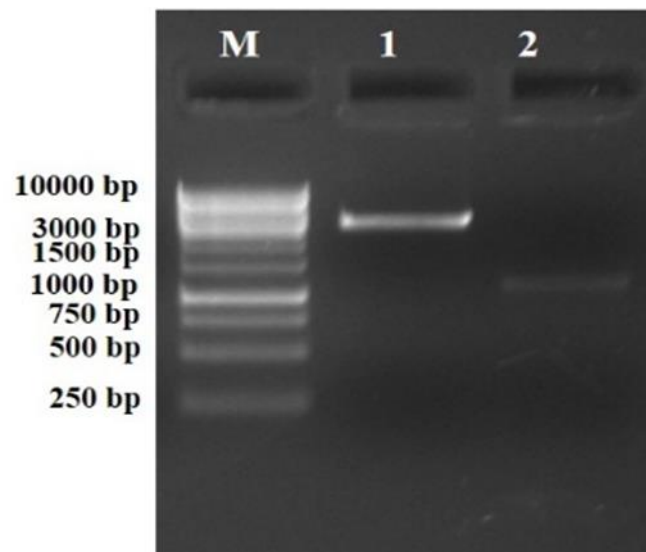


Figure 3. Restriction profile of the double-digested PCR product and control pBluescript vector. Lane M: 1 kb DNA ladder. Lane 1: ~3 kb fragment of pBS digested with *SpeI*+*HindIII*. Lane 2: ~1.078 kb fragment of purified PCR product. The PCR product was digested with *SpeI*+*HindIII*.

The ligated mixture was transformed into *E. coli* DH-5 α competent cells and five randomly picked white colonies were used for the plasmid isolation. The presence of the *phlD* gene was confirmed by restriction digestion with *SpeI*+*HindIII* enzymes that released the expected fragment of ~1 kb (Figure 4).

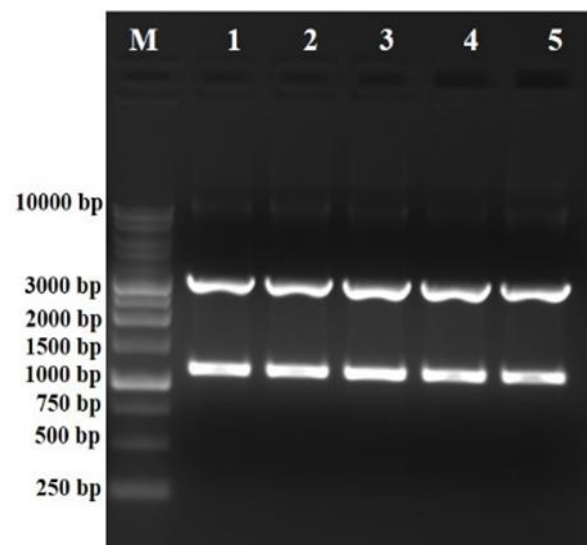


Figure 4. Screening and confirmation of positive putative clones by restriction digestion, respectively. Lanes 1–5: restriction digestion with *SpeI*+*HindIII* released a fragment of ~1.078 kb of the *phlD* gene and ~3 kb fragment of pBluescript (SK+) vector backbone.

Sanger sequencing of the cloned *phlD* was carried to check its identity and the results revealed that it consisted of 1078 nucleotides with an open reading frame of 1050 bp. Based on the blast results, the *phlD* gene was found to be of full-length coding for 349 amino acids. The cloned *phlD* gene showed considerable homology with the other known genes, indicating a common descent. The deduced amino acid sequence of 349 amino acids (~38.3 KDa) showed significant similarity with the homologs of PHLD (Figures 5 and 6).

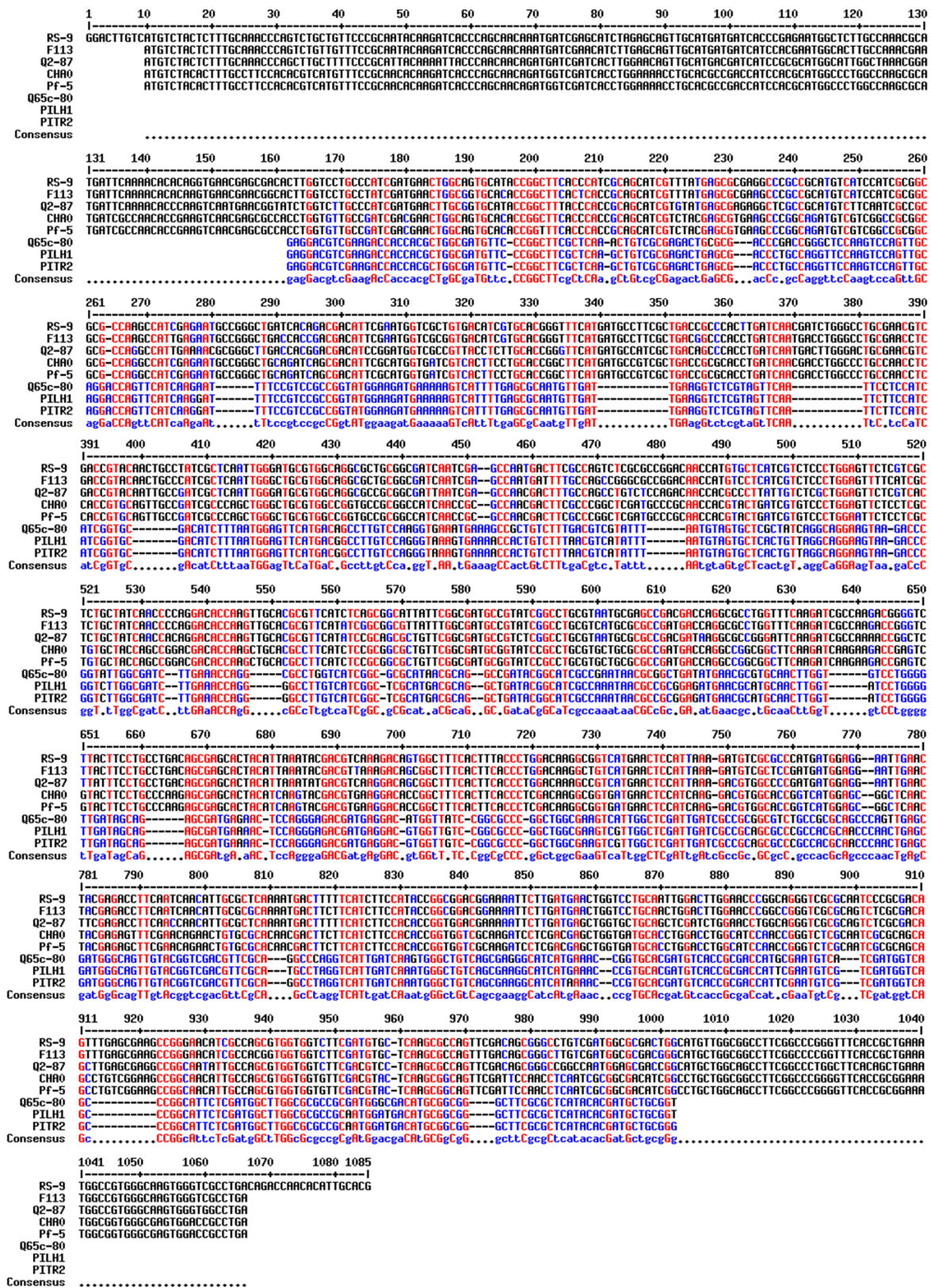


Figure 5. Pairwise sequence alignment of the cloned *phlD* gene (RS-9) with the reported DAPG producing *phlD* gene from *Pseudomonas* strains from the database (<http://multalin.toulouse.inra.fr/multalin/>, accessed on 15 March 2022). Our cloned *phlD* gene from the RS-9 strain showed homology with already reported *phlD* genes from *Pseudomonas* strain F113, Q2-87, CHAO, PF-5, Q65c-80, PILH1, and PITR2.

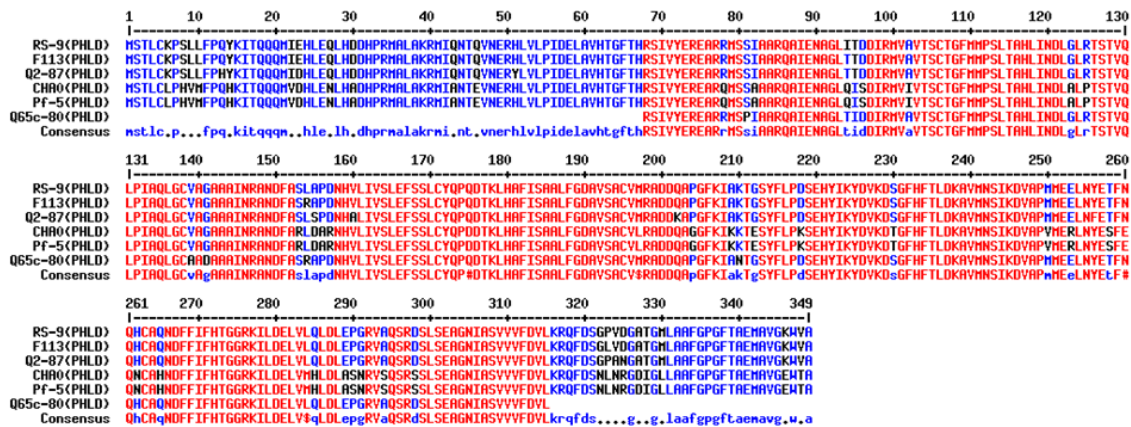


Figure 6. Pairwise sequence alignment of *Pseudomonas* spp. RS-9 PHLD protein with the PHLD protein from five *Pseudomonas* strains (<http://multalin.toulouse.inra.fr/multalin/>, accessed on 15 March 2022). The deduced amino acid sequence from the cloned *phlD* gene *Pseudomonas* strain RS-9 showed homology with the already reported PHLD protein from *Pseudomonas* strain F113, Q2-87, CHAO, and Pf-5.

The deduced amino acid sequence from *Pseudomonas* RS-9 was compared with type III PKSs from gram-positive bacteria and CHS/STS from plants. The functional roles of key amino acid residues found in type III PKSs/CHS/STS were found in PHLD proteins and other bacterial-type III PKSs (Figure 7), such as plant C169 (cysteine-169), responsible for the catalytic activities of plant CHSs, S158 in plants (serine-158), and Q166 in plants (glutamine-166), and were conserved in PHLD proteins. C135 (cysteine-135) and C195 (cysteine-195) played roles in substrate specificity and K180 (lysine-180), which are important for the enzymatic structure and function in plant-type III PKSs, and are replaced in the bacterial counterparts. Threonine, serine, and asparagine, respectively, replaced these amino acids in the PHLD sequences (Figure 7).

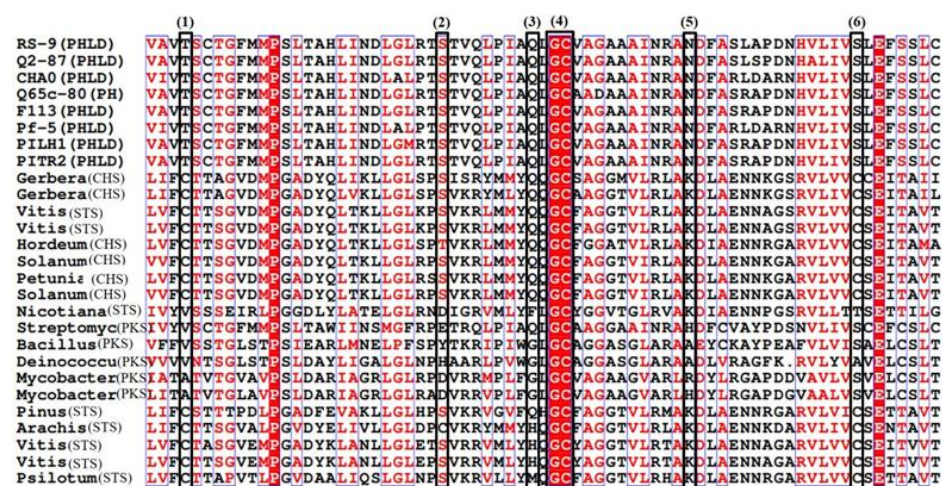


Figure 7. Alignment of predicted amino acid sequences for PHLD from various strains of *Pseudomonas* and type III polyketide synthase (PKS) from gram-positive bacteria and plant chalcone synthases/Stilbene synthase (CHS/STS). Conserved residues are indicated by boxes. (1) Cysteine (C135) from plant CHS implicated in substrate specificity and corresponding to threonine (T104) in PHLD. (2) Serine (S158) subunit contact site corresponding to S127 in PHLD. (3) Glutamine (Q166) residue conserved in most plant CHSs and corresponding to Q166 in the PKS of *Streptomyces griseus* and Q135 in PHLD proteins. (4) The glycine cysteine (GC) box corresponds to the conserved region with its catalytic cysteine residue. (5) Lysine (K180) residue, which corresponds to asparagine (N149) in PHLD, conserved strictly in the plant. (6) C195 involved in the product specificity in the plant CHS.

Analyses of the conserved domains and annotations were performed using InterProScan. The results revealed the presence of two InterPro domains viz. the chalcone/stilbene_synthases_N-terminal domain (37-200 a.a., IPR001099) and the chalcone/stilbene_synthases_C-terminal domain (213-344 a.a., IPR012328). These two domains belong to the Polyketide_synthase_type III InterPro family (IPR011141). A maximum likelihood (ML) tree was constructed to compare the phylogenetic relation of PHLD from *Pseudomonas* to Type III PKSs from bacteria and plants (PKS from other gram-positive bacteria and CHS/STS from plants). Upon comparison, eight PHLD sequences clustered into a separate group along with PKS from *Streptomyces griseus* (PKS). PKS from gram-positive bacteria and CHS/STS from plants also clustered in a separate group in the ML tree (Figure 8).

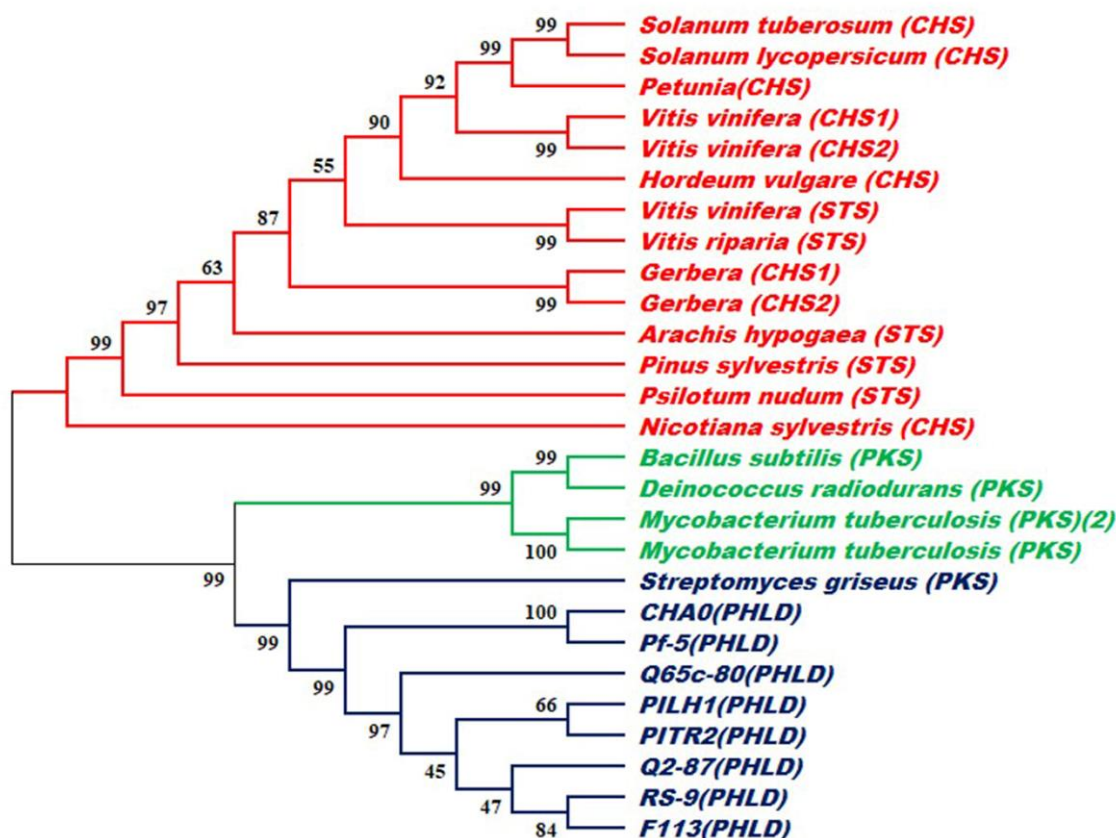


Figure 8. Diversity analysis between predicted amino acid sequences of PHLD from eight *Pseudomonas* strains and type III polyketide synthase from gram-positive bacteria (PKS) and plants (CHS/STS). The maximum likelihood (ML) tree was generated by the neighbor-joining method implemented in MEGA10.

The three-dimensional model of the PHLD protein using the deduced amino acid sequence of 349 amino acids was generated using the I-TASSER server (Figure 9) for the detailed structural analysis. The homology modeling of the initial structure was based on the template crystal structure of *Mycobacterium tuberculosis* polyketide synthase 11 (PKS11) (PDB entry 4JAP) [42]. The PHLD model had a C-score of 1.61 and a TM score of 0.94 ± 0.05 .

This initial model was refined using ModRefiner and Ramachandran plot analysis and the results of both analyses revealed that only 89.5% of residues were in the favored region, while 1% of residues were in the outlier region. The initial model was iteratively re-refined using Modloop until 0% of residues fell in the outlier region, 94.3% of residues fell in the favored region, and 5.7% in the allowed region (Figure 10). The predicted model was submitted to the Protein Model Database (PMDb) and was assigned the identifier PM0080923.

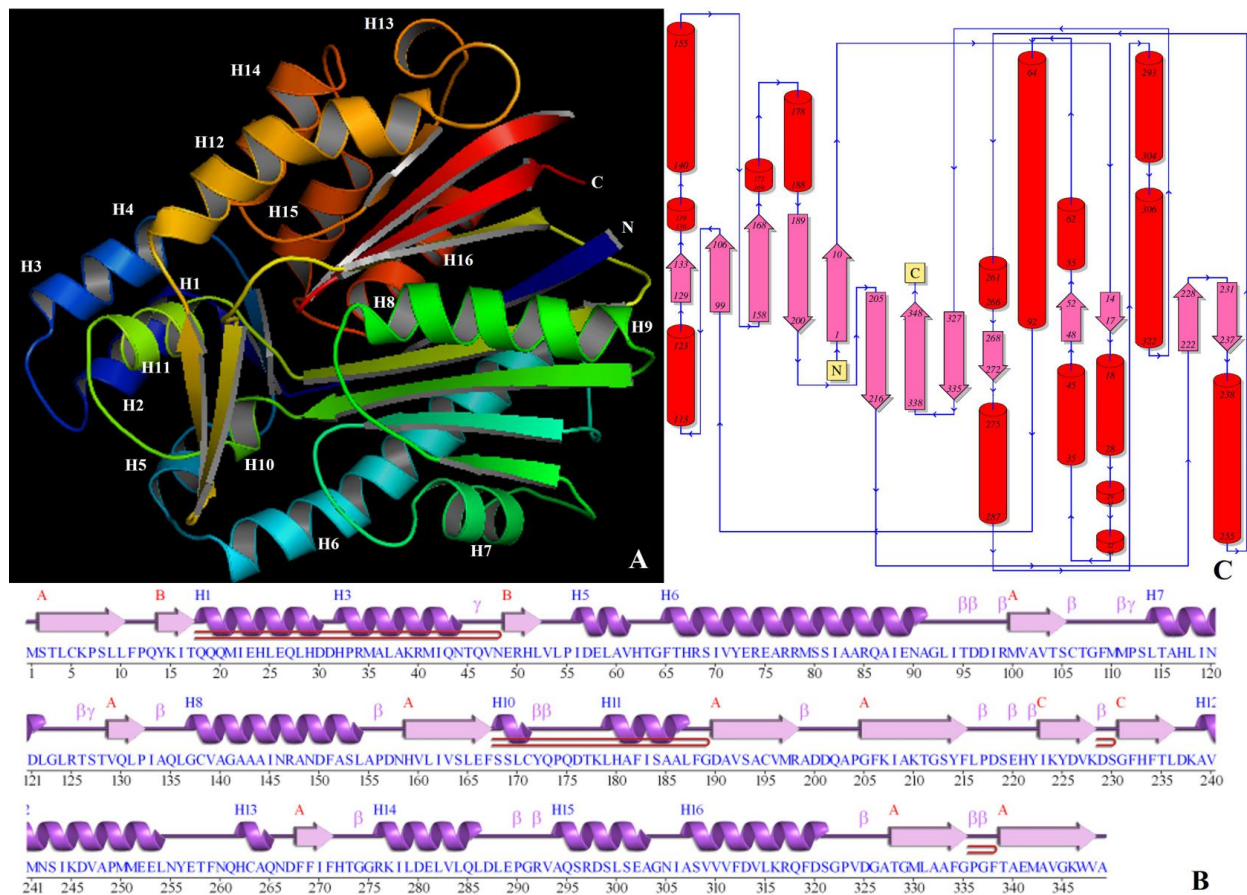


Figure 9. Structure of PHLD from *Pseudomonas* spp. (A) Stereo-ribbon diagram of the PHLD monomer (chain A) color-coded from the N-terminus (blue) to the C-terminus (red). Helices (H1–H16). (B) Diagram showing the secondary-structure elements of PHLD superimposed on its primary sequence. The labeling of the secondary-structure elements is in accordance with PDBsum (<http://www.ebi.ac.uk/pdbsum>): α -helices are labeled H1–H16, the β -strands are labeled β , β -turns and γ -turns are designated by their respective Greek letters (β , γ) and red loops indicate β -hairpins. (C) Topology of the PHLD protein showing the orientation of α -helices and β -strands.

The three-dimensional model generated by homology modeling was in accordance with the secondary structure predicted by PDBsum (Figure 9B,C). The PHLD secondary structure was dominated by the presence of α -helices (40.7%) followed by β -strands (26.1%) and 3-10 helices (2.6%). The PHLD structure revealed the presence of 3 beta sheets and 16 alpha-helices. β -sheet A contained 9 mixed β -strands with topology -3X -1X 2X 1 2X 3X -1X -1, β -sheet B and C contained 2 anti-parallel β -strands with topology 1 [43]. Protein also contained 16 α -helices viz; α 1 {Gln18–Gln27 (10 residues)}, α 2 {Leu28–Asp30 (3 residues)}, α 3 {His32–Arg34 (3 residues)}, α 4 {Met35–Asn44 (10 residues)}, α 5 {Ile56–Val61 (6 residues)}, α 6 {Phe65–Ala91 (27 residues)}, α 7 {Leu114–Leu122 (9 residues)}, α 8 {Gly137–Val139 (3 residues)}, α 9 {Ala140–Leu154 (15 residues)}, α 10 {Ser168–Cys171 (4 residues)}, α 11 {Leu179–Leu187 (9 residues)}, α 12 {Ala239–Leu254 (16 residues)}, α 13 {His262–Gln265 (4 residues)}, α 14 {Arg276–Leu286 (11 residues)}, α 15 {Ala294–Ala303 (10 residues)} and α 16 {Ala307–Ser321 (15 residues)}. The 4 β -hairpins of class 29:31, 20:22, 2:2 I, and 3:3 were identified [44]. The 14 helix–helix interactions, 12 H-H types (between α 1 and α 4, α 1, and α 5, α 1 and α 11, α 4 and α 11, α 6 and α 7, α 9, and α 16, α 11 and α 15, α 12 and α 13, α 12 and α 14, α 13 and α 14, α 14 and α 15, and α 15 and α 16), and 2 H-G type (α 5 and α 10 and α 6 and α 10) were identified.

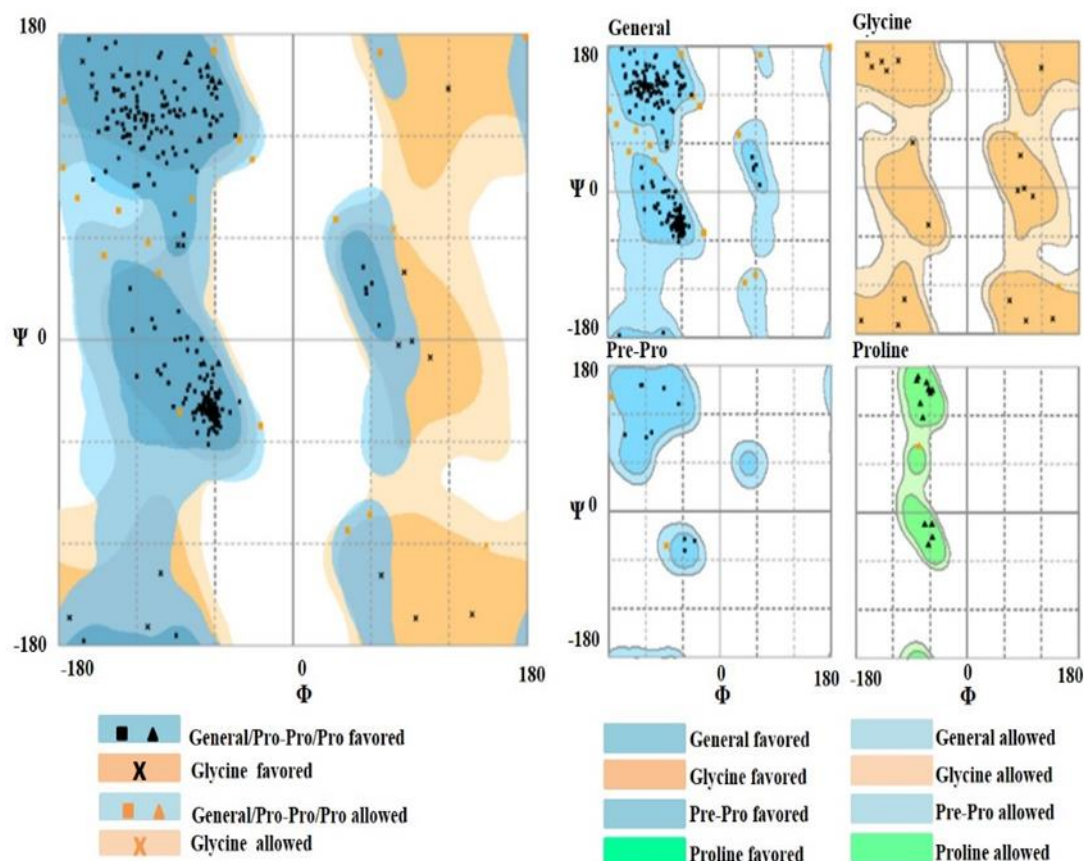


Figure 10. Stereochemical structure stability was analyzed using the Ramachandran plot analysis using RAMPAGE; 94.3% of residues fall in the favored region and 5.7% in the allowed region.

Two β - α - β motifs with 23 loops and 11 helices, and 56 loops and 42 helices participations were identified along with four β -bulges, one each of an anti-parallel classic type and anti-parallel wide type, and 2 anti-parallel G1 types were also identified. There are 21 β -turns in total belonging to 5 classes: I {(Thr95-Ile98), (Ser105-Gly108), (Tyr172-Gln175) and (Ser219-Tyr222)}; II{(Val324-Ala327) and (Gly335-Phe338)}; II'(Ile133-Leu136); IV{(Ile94-Asp97), (Ile98-Val101), (Met110-Ser113), (Arg125-Thr128), (Ala155-Asn158), (Cys171-Pro174), (Arg198-Asp201), (Leu216-Ser219), (Lys228-Gly231), (Thr273-Arg276), (Glu289-Arg292), (Pro336-Thr339) and (Gly291-Ala294)}; and VIII(His221-Lys224) [45]. Four γ turns of inverse types: (Thr45-Val47), (Met111-Ser113), (Thr126-Thr128), and (Thr273-Gly275) were also recognized.

4. Discussion

Special attention has been given to the antibiotic-producing fluorescent species of *Pseudomonas* due to their antibacterial [10,46], antifungal [47–50], and antiviral [51] abilities to control a wide variety of plant diseases. Advances in molecular techniques have also improved our potential to study the DAPG-producing antibacterial strains for their mechanisms of pathogen suppression and growth promotion. Breakthroughs in genomics [52–55] and transgenic [56,57] research to impart biotic/abiotic tolerance [58–60] or engineer traits in crops [61,62] have also driven the research in the field of biocontrol using DAPG producing strains. Genetic engineering approaches have been employed for the high-level production of phloroglucinol. Since the genetic background and metabolism of *Pseudomonas* have not been elucidated completely and the host does not respond well to genetic manipulation, the heterologous expression of *phlD* in *E. coli* is a great approach for increasing the accumulation of phloroglucinol in cultures [63–65].

DAPG is known to have antifungal properties and is produced by tandem activities of six genes viz. *phlA*, *phlB*, *phlC*, *phlD*, *phlE*, and *phlF*. These genes are organized as an operon onto a single nucleotide fragment of size ~ 6.5 kb. Among these six genes, *phlD* alone is important for the synthesis of MAPG. Although *phlA*, *phlB*, and *phlC* are also required for the synthesis of MAPG, *phlD* is the most essential. It has been proved that MAPG is synthesized only in the presence of *phlD* and in its absence, the cells converted exogenous MAPG to 2,4-DAPG but were unable to produce either compound themselves. This attribute makes *phlD* an important and useful marker of the genetic diversity and population structure among the 2,4-DAPG producers [14]. Thus, probes and primers specific for *phlD* have been used in combination with colony hybridization and polymerase chain reaction (PCR) to quantify the population sizes of 2,4-DAPG producers in the rhizosphere [11,66,67].

phlD shows a remarkable similarity to CHS/STS enzymes from plants. This is surprising because most of the microbial antibiotic enzymes are known to be synthesized via type I or type II PKSs [45,68–71]. Structural similarities between *phlD* and CHS/STS enzymes point to the common evolutionary descent and similarities in the roles they play during plant defense strongly support the instances of gene exchange between plants and bacteria [46,72]. The absence of the acyl carrier protein gene from the *phl* operon further confirms the similarity with the CHS/STS gene family. *Pseudomonas* spp. strain RS-9 was used for the isolation and cloning of the full-length *phlD* gene. The primers were designed using the *Pseudomonas fluorescens* (U41818) *phlD* gene sequence as a reference and *Pseudomonas* spp. strain RS-9 as the template. To amplify the full-length *phl* gene, we first standardized the PCR conditions. A gradient PCR was set in a temperature range of 50 °C to 60 °C to optimize the T_m for the reaction. At a lower T_m , multiple bands were obtained and at a very high T_m , faint amplification was obtained. The optimum amplification of ~1 kb for the *phlD* gene was obtained at 55 °C. This amplicon was restricted, purified, and ligated to the pBluescript vector and transformed into *E. coli* cells.

The cloned *phlD* gene through our investigation was confirmed by Sanger sequencing and it consisted of 1078 nucleotides with an open reading frame from 10 to 1059. The longest ORF of the *phlD* gene was found to be 1050 bp. Based on the blast results, the cloned *phlD* gene was found to be full-length, coding for 349 amino acids. This is consistent with the other reports [73] (Figure 5) on the length of amino acid coding *phl* genes. The cloned *phlD* gene showed 93% homology with *phlD* genes from different *Pseudomonas* strains, such as *Pseudomonas* sp. Q12-87, *Pseudomonas* sp. K96.27, *Pseudomonas* sp. P1TR2, *Pseudomonas* sp. Q37-87, *Pseudomonas* sp. 12. The deduced amino acid sequence of 349 amino acids (~38.3 kDa) showed 97% similarity with the homologs of PHLD [73]. The *phlD* gene is of utmost importance to the DAPG gene cluster as MAPG synthesis does not occur without it.

The deduced amino acid sequence of the cloned *phlD* gene consisting of 349 amino acids was aligned pairwise with the *Pseudomonas fluorescens* (U41818) PHLD protein. The alignment revealed that there were few mutations in the protein sequence of the cloned gene. These mutations were authentic as we amplified and cloned the gene using high-fidelity Phusion *Taq* polymerase. Since this *Taq* polymerase has 3' of proofreading activity, the chances of mis-amplifying or incorporating wrong bases are meager. These mutations need further characterization by site-directed mutagenesis.

A comparison of the deduced amino acid sequence from *Pseudomonas* RS-9, type III PKS from plants (CHS/STS), and other gram-positive bacteria indicated that PHLD and plant CHSs displayed common features. Comparison of the active site region indicated replacements of C135, C195, and K180 with threonine, serine, and asparagine that might have influenced their substrate specificities. Lysine and asparagine codons differ only at the third nucleotide position, and a single transversion can yield an asparagine instead of a lysine. The cluster analysis clearly distinguished between PhlD and plant CHS/STS by clustering them into separate groups [74–76]. Type III PKS from gram-positive bacteria clustered between CHS/STS from plants and PHLD from eight *Pseudomonas* strains. PKS closest to PHLD was the *Streptomyces gresius* PKS based on cluster analysis. The possibility that type III PKSs from fluorescent pseudomonads, gram-positive bacteria, and higher plants arose

independently and may represent convergent evolution of the key enzymes involved in the biosynthesis of secondary metabolites as speculated earlier [46,73], corroborating our results of the cluster analysis.

The three-dimensional structure of the PHLD protein predicted using the I-TASSER server was based on the template crystal structure of *Mycobacterium tuberculosis* polyketide synthase 11 (PKS11) (PDB entry 4JAP) [42]. The PHLD model had an excellent C-score of 1.61 indicating a good quality model. C-score ranged from -5 to 2 and this higher value indicates the high quality of the model. Similarly, a TM score >0.5 indicated a model of correct topology, and a TM score <0.17 meant a random similarity. A TM score of 0.94 ± 0.05 for PHLD indicates the precision of the predicted topology. Moreover, $>90\%$ residues (94.3% residues) in the favored region of the Ramachandran plot reaffirmed the stereochemical stability of the generated refined molecule.

5. Conclusions

Pseudomonas strains have been used as potent biocontrol agents for controlling plant diseases because of the production of metabolites with antibiotic properties [77]. Amongst them, fluorescent pseudomonads are suitable for application as biocontrol agents and are best-characterized by biocontrol PGPR [78]. The biocontrol property of *Pseudomonas* is attributed to the synthesis of phloroglucinol—a secondary metabolite with antibiotic properties—produced by genes encoded by the *phl* operon. The *phlD* gene present in the *phl* operon is singularly involved in the synthesis of MAPG, which is processed into phloroglucinol. Though *PhlD* exhibits condensing activity on malonyl CoA to produce phloroglucinol; the substrate specificity of the enzyme is not limited to malonyl CoA compared to other type III PKS enzymes. It also catalyzes “C4–C12 aliphatic acyl-CoAs and phenylacetyl-CoA” as substrates to form tri- to heptaketide pyrones [25]. The same is evidenced by the homology modelling of *PhlD* that reveals the presence of a buried tunnel that protrudes out of the active site to accommodate the binding of acyl-CoAs. Structural details revealed from our findings can be used for targeted mutagenesis and rational designs to successfully alter the substrate specificity of *PhlD* to produce derivatized products with higher potency for antibiosis. Since, *phlD* is the first committed step of DAPG biosynthesis, targeting substrate specificity of *PhlD* would be a prudent way to enhance the biocontrol activities of *Pseudomonas* spp. that otherwise are present as long-lasting indigenous communities in several agro-ecosystems to augment the capability to protect the plant root system from numerous soil-borne plant diseases. Our results of cloning and structural delineation of *phlD* will provide novel strategies for combinatorial biosynthesis of natural but pharmaceutically important metabolites with enhanced antibacterial and biocontrol effects.

Author Contributions: R.R., R.S., S.K.P. and P.K.D. conceptualized the work and designed the experiments. P.G. and P.K.D. carried out the research. R.R., P.K.D., T.D.S., R.S. and S.K.P. analyzed the data. P.G. wrote the manuscript (first draft) with input from all authors. R.R. and P.K.D. edited the manuscript. All authors have read and agreed to the published version of the manuscript.

Funding: This research received no external funding.

Institutional Review Board Statement: This is NIPB publication number NIPB/2022/Res-35.

Informed Consent Statement: Not applicable.

Data Availability Statement: Not applicable.

Acknowledgments: The present study was carried out by DBT, GoI, grant to R.R. and as an in-house RPP project to R.R. and P.K.D. (RPP—Sanction no. 7–5/2010-IC-IV) by the Indian Council of Agricultural Research (ICAR), New Delhi, India. Financial support from ICAR-NPFGGM (RR, PKD) and a scholarship to P.G. is acknowledged. This is an NIPB publication (number NIPB/2022/Res-35).

Conflicts of Interest: The authors declare no conflict of interest.

References

1. Kloepper, J.; Lifshitz, R.; Schroth, M. *Pseudomonas Inoculants to Benefit Plant Protection*; Institute for Scientific Information: Philadelphia, PA, USA, 1988.
2. Troppens, D.; Moynihan, J.; Barret, M.; O’Gara, F.; Morrissey, J. *Molecular Microbial Ecology of the Rhizosphere*; John Wiley and Sons, Ltd.: Hoboken, NJ, USA, 2013.
3. Mandryk-Litvinkovich, M.N.; Muratova, A.A.; Nosonova, T.L.; Evdokimova, O.V.; Valentovich, L.N.; Titok, M.A.; Kolomiets, E.I. Molecular Genetic Analysis of Determinants Defining Synthesis of 2,4-Diacetylphloroglucinol by *Pseudomonas Brassicacearum* BIM B-446 Bacteria. *Appl. Biochem. Microbiol.* **2017**, *53*, 31–39. [[CrossRef](#)]
4. Thomashow, L.; Weller, D. Current Concepts in the Use of Introduced Bacteria for Biological Disease Control: Mechanisms and Antifungal Metabolites. In *Plant-Microbe Interactions*; Springer US: Boston, MA, USA, 1996; pp. 187–235.
5. van Loon, L.C.; Bakker, P.A.H.M.; Pieterse, C.M.J. Systemic Resistance Induced By Rhizosphere Bacteria. *Annu. Rev. Phytopathol.* **1998**, *36*, 453–483. [[CrossRef](#)]
6. Almario, J.; Moënne-Loccoz, Y.; Muller, D. Monitoring of the Relation between 2,4-Diacetylphloroglucinol-Producing *Pseudomonas* and *Thielaviopsis Basicola* Populations by Real-Time PCR in Tobacco Black Root-Rot Suppressive and Conducive Soils. *Soil Biol. Biochem.* **2013**, *57*, 144–155. [[CrossRef](#)]
7. Haichar, F.; Fochesato, S.; Achouak, W. Host Plant Specific Control of 2,4-Diacetylphloroglucinol Production in the Rhizosphere. *Agronomy* **2013**, *3*, 621–631. [[CrossRef](#)]
8. Zhou, T.-T.; Li, C.-Y.; Chen, D.; Wu, K.; Shen, Q.-R.; Shen, B. PhIF– Mutant of *Pseudomonas Fluorescens* J2 Improved 2,4-DAPG Biosynthesis and Biocontrol Efficacy against Tomato Bacterial Wilt. *Biol. Control* **2014**, *78*, 1–8. [[CrossRef](#)]
9. Bonsall, R.F.; Weller, D.M.; Thomashow, L.S. Quantification of 2,4-Diacetylphloroglucinol Produced by Fluorescent *Pseudomonas* Spp. In Vitro and in the Rhizosphere of Wheat. *Appl. Environ. Microbiol.* **1997**, *63*, 951–955. [[CrossRef](#)]
10. Duffy, B.K.; Défago, G. Zinc Improves Biocontrol of Fusarium Crown and Root Rot of Tomato by *Pseudomonas fluorescens* and Represses the Production of Pathogen Metabolites Inhibitory to Bacterial Antibiotic Biosynthesis. *Phytopathology* **1997**, *87*, 1250–1257. [[CrossRef](#)]
11. Raaijmakers, J.M.; Weller, D.M. Natural Plant Protection by 2,4-Diacetylphloroglucinol-Producing *Pseudomonas* Spp. in Take-All Decline Soils. *Mol. Plant-Microbe Interact.* **1998**, *11*, 144–152. [[CrossRef](#)]
12. Sulaiman, M.; Jannat, K.; Nissapatorn, V.; Rahmatullah, M.; Paul, A.K.; de Lourdes Pereira, M.; Rajagopal, M.; Suleiman, M.; Butler, M.S.; bin Break, M.K.; et al. Antibacterial and Antifungal Alkaloids from Asian Angiosperms: Distribution, Mechanisms of Action, Structure-Activity, and Clinical Potentials. *Antibiotics* **2022**, *11*, 1146. [[CrossRef](#)]
13. Hansanant, N.; Smith, L. Occidiofungin: Actin Binding as a Novel Mechanism of Action in an Antifungal Agent. *Antibiotics* **2022**, *11*, 1143. [[CrossRef](#)]
14. Delany, I.; Sheehan, M.M.; Fenton, A.; Bardin, S.; Aarons, S.; O’Gara, F. Regulation of Production of the Antifungal Metabolite 2,4-Diacetylphloroglucinol in *Pseudomonas Fluorescens* F113: Genetic Analysis of PhIF as a Transcriptional Repressor The GenBank Accession Number for the Sequence Reported in This Paper Is AF129856. *Microbiology* **2000**, *146*, 537–546. [[CrossRef](#)] [[PubMed](#)]
15. Keel, C. Suppression of Root Diseases by *Pseudomonas fluorescens* CHA0: Importance of the Bacterial Secondary Metabolite 2,4-Diacetylphloroglucinol. *Mol. Plant-Microbe Interact.* **1992**, *5*, 4. [[CrossRef](#)]
16. Mavrodi, O.V.; McSpadden Gardener, B.B.; Mavrodi, D.V.; Bonsall, R.F.; Weller, D.M.; Thomashow, L.S. Genetic Diversity of *PhlD* from 2,4-Diacetylphloroglucinol-Producing Fluorescent *Pseudomonas* spp. *Phytopathology* **2001**, *91*, 35–43. [[CrossRef](#)] [[PubMed](#)]
17. Voisard, C.; Bull, C.; Keel, C.; Laville, J.; Maurhofer, M.; Schnider, U.; Dfago, G.; Haas, D. Biocontrol of Root Diseases By *Pseudomonas Fluorescens* CHA0: Current Concepts and Experimental Approaches. In *Molecular Ecology of Rhizosphere Microorganisms*; Wiley-VCH Verlag GmbH: Weinheim, Germany, 1994; pp. 67–89.
18. Whistler, C.A.; Corbell, N.A.; Sarniguet, A.; Ream, W.; Loper, J.E. The Two-Component Regulators GacS and GacA Influence Accumulation of the Stationary-Phase Sigma Factor σ^S and the Stress Response in *Pseudomonas Fluorescens* Pf-5. *J. Bacteriol.* **1998**, *180*, 6635–6641. [[CrossRef](#)] [[PubMed](#)]
19. Yuan, Z.; Cang, S.; Matsufuji, M.; Nakata, K.; Nagamatsu, Y.; Yoshimoto, A. High Production of Pyoluteorin and 2,4-Diacetylphloroglucinol by *Pseudomonas Fluorescens* S272 Grown on Ethanol as a Sole Carbon Source. *J. Ferment. Bioeng.* **1998**, *86*, 559–563. [[CrossRef](#)]
20. Duffy, B.K.; Défago, G. Environmental Factors Modulating Antibiotic and Siderophore Biosynthesis by *Pseudomonas Fluorescens* Biocontrol Strains. *Appl. Environ. Microbiol.* **1999**, *65*, 2429–2438. [[CrossRef](#)]
21. Shanahan, P.; O’Sullivan, D.J.; Simpson, P.; Glennon, J.D.; O’Gara, F. Isolation of 2,4-Diacetylphloroglucinol from a Fluorescent *Pseudomonad* and Investigation of Physiological Parameters Influencing Its Production. *Appl. Environ. Microbiol.* **1992**, *58*, 353–358. [[CrossRef](#)]
22. Biessy, A.; Fillion, M. Phloroglucinol Derivatives in Plant-Beneficial *Pseudomonas* spp.: Biosynthesis, Regulation, and Functions. *Metabolites* **2021**, *11*, 182. [[CrossRef](#)]
23. Shimizu, Y.; Ogata, H.; Goto, S. Type III Polyketide Synthases: Functional Classification and Phylogenomics. *ChemBioChem* **2017**, *18*, 50–65. [[CrossRef](#)]
24. Achkar, J.; Xian, M.; Zhao, H.; Frost, J.W. Biosynthesis of Phloroglucinol. *J. Am. Chem. Soc.* **2005**, *127*, 5332–5333. [[CrossRef](#)]

25. Zha, W.; Rubin-Pitel, S.B.; Zhao, H. Characterization of the Substrate Specificity of PhlD, a Type III Polyketide Synthase from *Pseudomonas Fluorescens*. *J. Biol. Chem.* **2006**, *281*, 32036–32047. [[CrossRef](#)] [[PubMed](#)]
26. Gupta, P.; Rai, R.; Dash, P.K. Isolation, Cloning and Characterization of PhlA Gene from an Indigenous *Pseudomonas* Strain from Indian Soil. *Int. J. Trop. Agric.* **2015**, *33*, 3195–3200.
27. Dash, P.; Gupta, P.; Panwar, B.S.; Rai, R. Isolation, Cloning and Characterization of PhlB Gene from an Indian Strain of Gram Negative Soil Bacteria *Pseudomonas Fluorescens*. *Indian J. Exp. Biol.* **2020**, *58*, 412–419.
28. Gupta, P.; Karthik, K.; Sreevathsa, R.; Rai, R.; Dash, P.K. Cloning and Characterization of Phloroglucinol Biosynthetic Gene PhlC from An Indian Strain of *Pseudomonas Fluorescens*. *Indian J. Exp. Biol.* **2022**, *60*, 607–614. [[CrossRef](#)]
29. Rai, R.; Srinivasamurthy, R.; Dash, P.K.; Gupta, P. Isolation, Characterization and Evaluation of the Biocontrol Potential of *Pseudomonas Protegens* RS-9 against *Ralstonia Solanacearum* in Tomato. *Indian J. Exp. Biol.* **2017**, *55*, 595–603.
30. Katoh, K.; Standley, D.M. MAFFT Multiple Sequence Alignment Software Version 7: Improvements in Performance and Usability. *Mol. Biol. Evol.* **2013**, *30*, 772–780. [[CrossRef](#)]
31. Robert, X.; Gouet, P. Deciphering Key Features in Protein Structures with the New ENDScript Server. *Nucleic Acids Res.* **2014**, *42*, W320–W324. [[CrossRef](#)]
32. Jones, P.; Binns, D.; Chang, H.-Y.; Fraser, M.; Li, W.; McAnulla, C.; McWilliam, H.; Maslen, J.; Mitchell, A.; Nuka, G.; et al. InterProScan 5: Genome-Scale Protein Function Classification. *Bioinformatics* **2014**, *30*, 1236–1240. [[CrossRef](#)]
33. Sievers, F.; Wilm, A.; Dineen, D.; Gibson, T.J.; Karplus, K.; Li, W.; Lopez, R.; McWilliam, H.; Remmert, M.; Söding, J.; et al. Fast, Scalable Generation of High-Quality Protein Multiple Sequence Alignments Using Clustal Omega. *Mol. Syst. Biol.* **2011**, *7*, 539. [[CrossRef](#)]
34. Kumar, S.; Stecher, G.; Li, M.; Nnyaz, C.; Tamura, K. MEGA X: Molecular Evolutionary Genetics Analysis across Computing Platforms. *Mol. Biol. Evol.* **2018**, *35*, 1547–1549. [[CrossRef](#)]
35. Guindon, S.; Dufayard, J.F.; Lefort, V.; Anisimova, M.; Hordijk, W.; Gascuel, O. New Algorithms and Methods to Estimate Maximum-Likelihood Phylogenies: Assessing the Performance of PhyML 3.0. *Syst. Biol.* **2010**, *59*, 307–321. [[CrossRef](#)] [[PubMed](#)]
36. Zhang, Y. I-TASSER: Fully Automated Protein Structure Prediction in CASP8. *Proteins Struct. Funct. Bioinform.* **2009**, *77*, 100–113. [[CrossRef](#)] [[PubMed](#)]
37. Lovell, S.C.; Davis, I.W.; Arendall, W.B.; de Bakker, P.I.W.; Word, J.M.; Prisant, M.G.; Richardson, J.S.; Richardson, D.C. Structure Validation by α Geometry: ϕ , ψ and $C\beta$ Deviation. *Proteins Struct. Funct. Bioinform.* **2003**, *50*, 437–450. [[CrossRef](#)] [[PubMed](#)]
38. Fiser, A.; Sali, A. ModLoop: Automated Modeling of Loops in Protein Structures. *Bioinformatics* **2003**, *19*, 2500–2501. [[CrossRef](#)] [[PubMed](#)]
39. Laskowski, R.A. PDBsum More: New Summaries and Analyses of the Known 3D Structures of Proteins and Nucleic Acids. *Nucleic Acids Res.* **2004**, *33*, D266–D268. [[CrossRef](#)] [[PubMed](#)]
40. Laskowski, R.A.; MacArthur, M.W.; Moss, D.S.; Thornton, J.M. PROCHECK: A Program to Check the Stereochemical Quality of Protein Structures. *J. Appl. Crystallogr.* **1993**, *26*, 283–291. [[CrossRef](#)]
41. Castrignano, T. The PMDB Protein Model Database. *Nucleic Acids Res.* **2006**, *34*, D306–D309. [[CrossRef](#)]
42. Gokulan, K.; O’Leary, S.E.; Russell, W.K.; Russell, D.H.; Lalgondar, M.; Begley, T.P.; Ioerger, T.R.; Sacchettini, J.C. Crystal Structure of Mycobacterium Tuberculosis Polyketide Synthase 11 (PKS11) Reveals Intermediates in the Synthesis of Methyl-Branched Alkylpyrones. *J. Biol. Chem.* **2013**, *288*, 16484–16494. [[CrossRef](#)]
43. Richardson, J.S. The Anatomy and Taxonomy of Protein Structure. *Adv. Protein Chem.* **1981**, *34*, 167–339.
44. Sibanda, B.L.; Blundell, T.L.; Thornton, J.M. Conformation of β -Hairpins in Protein Structures. *J. Mol. Biol.* **1989**, *206*, 759–777. [[CrossRef](#)]
45. Hutchinson, C.R.; Fujii, I. POLYKETIDE SYNTHASE GENE MANIPULATION: A Structure-Function Approach in Engineering Novel Antibiotics. *Annu. Rev. Microbiol.* **1995**, *49*, 201–238. [[CrossRef](#)] [[PubMed](#)]
46. Cook, R.J.; Thomashow, L.S.; Weller, D.M.; Fujimoto, D.; Mazzola, M.; Banger, G.; Kim, D.S. Molecular Mechanisms of Defense by Rhizobacteria against Root Disease. *Proc. Natl. Acad. Sci. USA* **1995**, *92*, 4197–4201. [[CrossRef](#)] [[PubMed](#)]
47. Fenton, A.M.; Stephens, P.M.; Crowley, J.; O’Callaghan, M.; O’Gara, F. Exploitation of Gene(s) Involved in 2,4-Diacetylphloroglucinol Biosynthesis to Confer a New Biocontrol Capability to a *Pseudomonas* Strain. *Appl. Environ. Microbiol.* **1992**, *58*, 3873–3878. [[CrossRef](#)] [[PubMed](#)]
48. Sharifi-Tehrani, A.; Zala, M.; Natsch, A.; Moënné-Loccoz, Y.; Défago, G. Biocontrol of Soil-Borne Fungal Plant Diseases by 2,4-Diacetylphloroglucinol-Producing Fluorescent *Pseudomonads* with Different Restriction Profiles of Amplified 16S rDNA. *Eur. J. Plant Pathol.* **1998**, *104*, 631–643. [[CrossRef](#)]
49. Stutz, E.W. Naturally Occurring Fluorescent *Pseudomonads* Involved in Suppression of Black Root Rot of Tobacco. *Phytopathology* **1986**, *76*, 181. [[CrossRef](#)]
50. Tamietti, G.; Ferraris, L.; Matta, A.; Abbattista Gentile, I. Physiological Responses of Tomato Plants Grown in Fusarium Suppressive Soil. *J. Phytopathol.* **1993**, *138*, 66–76. [[CrossRef](#)]
51. Suresh, P.; Rekha, M.; Gomathinayagam, S.; Ramamoorthy, V.; Sharma, M.P.; Sakthivel, P.; Sekar, K.; Valan Arasu, M.; Shanmugaiah, V. Characterization and Assessment of 2, 4-Diacetylphloroglucinol (DAPG)-Producing *Pseudomonas Fluorescens* VSMKU3054 for the Management of Tomato Bacterial Wilt Caused by *Ralstonia Solanacearum*. *Microorganisms* **2022**, *10*, 1508. [[CrossRef](#)]

52. Dash, P.K.; Cao, Y.; Jailani, A.K.; Gupta, P.; Venglat, P.; Xiang, D.; Rai, R.; Sharma, R.; Thirunavukkarasu, N.; Abdin, M.Z.; et al. Genome-Wide Analysis of Drought Induced Gene Expression Changes in Flax (*Linum usitatissimum*). *GM Crops Food* **2014**, *5*, 106–119. [[CrossRef](#)] [[PubMed](#)]
53. Wang, Z.; Hobson, N.; Galindo, L.; Zhu, S.; Shi, D.; McDill, J.; Yang, L.; Hawkins, S.; Neutelings, G.; Datla, R.; et al. The Genome of Flax (*Linum Usitatissimum*) Assembled *de Novo* from Short Shotgun Sequence Reads. *Plant J.* **2012**, *72*, 461–473. [[CrossRef](#)]
54. Dash, P.K.; Rai, R.; Mahato, A.K.; Gaikwad, K.; Singh, N.K. Transcriptome Landscape at Different Developmental Stages of a Drought Tolerant Cultivar of Flax (*Linum Usitatissimum*). *Front. Chem.* **2017**, *5*, 82. [[CrossRef](#)] [[PubMed](#)]
55. Dash, P.K.; Gupta, P.; Pradhan, S.K.; Shasany, A.K.; Rai, R. Analysis of Homologous Regions of Small RNAs MIR397 and MIR408 Reveals the Conservation of Microsynteny among Rice Crop-Wild Relatives. *Cells* **2022**, *11*, 3461. [[CrossRef](#)] [[PubMed](#)]
56. Shivakumara, T.N.; Sreevathsa, R.; Dash, P.K.; Sheshshayee, M.S.; Papolu, P.K.; Rao, U.; Tuteja, N.; UdayaKumar, M. Overexpression of Pea DNA Helicase 45 (PDH45) Imparts Tolerance to Multiple Abiotic Stresses in Chili (*Capsicum annum L.*). *Sci. Rep.* **2017**, *7*, 2760. [[CrossRef](#)] [[PubMed](#)]
57. Kesiraju, K.; Tyagi, S.; Mukherjee, S.; Rai, R.; Singh, N.K.; Sreevathsa, R.; Dash, P.K. An Apical Meristem-Targeted in Planta Transformation Method for the Development of Transgenics in Flax (*Linum Usitatissimum*): Optimization and Validation. *Front. Plant Sci.* **2021**, *11*, 562056. [[CrossRef](#)]
58. Gupta, P.; Dash, P.K. Precise Method of in Situ Drought Stress Induction in Flax (*Linum usitatissimum*) for RNA Isolation towards down-Stream Analysis. *Ann. Agric. Res.* **2015**, *36*, 10–17.
59. Bastia, R.; Pandit, E.; Sanghamitra, P.; Barik, S.R.; Nayak, D.K.; Sahoo, A.; Moharana, A.; Meher, J.; Dash, P.K.; Raj, R.; et al. Association Mapping for Quantitative Trait Loci Controlling Superoxide Dismutase, Flavonoids, Anthocyanins, Carotenoids, γ -Oryzanol and Antioxidant Activity in Rice. *Agronomy* **2022**, *12*, 3036. [[CrossRef](#)]
60. Pradhan, K.C.; Pandit, E.; Mohanty, S.P.; Moharana, A.; Sanghamitra, P.; Meher, J.; Jena, B.K.; Dash, P.K.; Behera, L.; Mohapatra, P.M.; et al. Development of Broad Spectrum and Durable Bacterial Blight Resistant Variety through Pyramiding of Four Resistance Genes in Rice. *Agronomy* **2022**, *12*, 1903. [[CrossRef](#)]
61. Sedeek, K.E.M.; Mahas, A.; Mahfouz, M. Plant Genome Engineering for Targeted Improvement of Crop Traits. *Front. Plant Sci.* **2019**, *10*, 114. [[CrossRef](#)]
62. Pradhan, S.K.; Pandit, E.; Pawar, S.; Bharati, B.; Chatopadhyay, K.; Singh, S.; Dash, P.; Reddy, J.N. Association Mapping Reveals Multiple QTLs for Grain Protein Content in Rice Useful for Biofortification. *Mol. Genet. Genom.* **2019**, *294*, 963–983. [[CrossRef](#)]
63. Yang, F.; Cao, Y. Biosynthesis of Phloroglucinol Compounds in Microorganisms—Review. *Appl. Microbiol. Biotechnol.* **2012**, *93*, 487–495. [[CrossRef](#)]
64. Rao, G.; Lee, J.-K.; Zhao, H. Directed Evolution of Phloroglucinol Synthase PhID with Increased Stability for Phloroglucinol Production. *Appl. Microbiol. Biotechnol.* **2013**, *97*, 5861–5867. [[CrossRef](#)]
65. Yu, S.; Guo, L.; Zhao, L.; Chen, Z.; Huo, Y. Metabolic Engineering of *E. Coli* for Producing Phloroglucinol from Acetate. *Appl. Microbiol. Biotechnol.* **2020**, *104*, 7787–7799. [[CrossRef](#)] [[PubMed](#)]
66. Raaijmakers, J.M.; Weller, D.M.; Thomashow, L.S. Frequency of Antibiotic-Producing *Pseudomonas* Spp. in Natural Environments. *Appl. Environ. Microbiol.* **1997**, *63*, 881–887. [[CrossRef](#)] [[PubMed](#)]
67. Picard, C.; di Cello, F.; Ventura, M.; Fani, R.; Guckert, A. Frequency and Biodiversity of 2,4-Diacetylphloroglucinol-Producing Bacteria Isolated from the Maize Rhizosphere at Different Stages of Plant Growth. *Appl. Environ. Microbiol.* **2000**, *66*, 948–955. [[CrossRef](#)] [[PubMed](#)]
68. Donadio, S.; Staver, M.; McAlpine, J.; Swanson, S.; Katz, L. Modular Organization of Genes Required for Complex Polyketide Biosynthesis. *Science (1979)* **1991**, *252*, 675–679. [[CrossRef](#)]
69. Katz, L.; Donadio, S. POLYKETIDE SYNTHESIS: Prospects for Hybrid Antibiotics. *Annu. Rev. Microbiol.* **1993**, *47*, 875–912. [[CrossRef](#)] [[PubMed](#)]
70. Nowak-Thompson, B.; Gould, S.J.; Loper, J.E. Identification and Sequence Analysis of the Genes Encoding a Polyketide Synthase Required for Pyoluteorin Biosynthesis in *Pseudomonas Fluorescens* Pf-5. *Gene* **1997**, *204*, 17–24. [[CrossRef](#)]
71. McDaniel, R.; Ebert-Khosla, S.; Hopwood, D.A.; Khosla, C. Engineered Biosynthesis of Novel Polyketides. *Science (1979)* **1993**, *262*, 1546–1550. [[CrossRef](#)]
72. Bangera, M.G.; Weller, D.M.; Thomshaw, L.S. Genetic Analysis of the 2,4-Diacetylphloroglucinol Biosynthetic Locus from *Pseudomonas Fluorescens* Q2-87. In *Advances in Molecular Genetics of Plant-Microbe Interactions*; Daniels, M., Downie, J., Osbourn, A., Eds.; Kluwer Academic Publishers: Dordrecht, The Netherlands, 1994.
73. Bangera, M.G.; Thomashow, L.S. Identification and Characterization of a Gene Cluster for Synthesis of the Polyketide Antibiotic 2,4-Diacetylphloroglucinol from *Pseudomonas fluorescens* Q2-87. *J. Bacteriol.* **1999**, *181*, 3155–3163. [[CrossRef](#)]
74. Ramette, A.; Moëne-Loccoz, Y.; Défago, G. Polymorphism of the Polyketide Synthase Gene *PhID* in Biocontrol Fluorescent *Pseudomonads* Producing 2,4-Diacetylphloroglucinol and Comparison of PhID with Plant Polyketide Synthases. *Mol. Plant-Microbe Interact.* **2001**, *14*, 639–652. [[CrossRef](#)]
75. Tropf, S.; Lanz, T.; Rensing, S.A.; Schrder, J.; Schrder, G. Evidence That Stilbene Synthases Have Developed from Chalcone Synthases Several Times in the Course of Evolution. *J. Mol. Evol.* **1994**, *38*, 610–618. [[CrossRef](#)]
76. de Luca, D.; Lauritano, C. In Silico Identification of Type III PKS Chalcone and Stilbene Synthase Homologs in Marine Photosynthetic Organisms. *Biology* **2020**, *9*, 110. [[CrossRef](#)] [[PubMed](#)]

77. Höfte, M. *The Use of Pseudomonas spp. as Bacterial Biocontrol Agents to Control Plant Disease*; Burleigh Dodds: Cambridge, UK, 2021.
78. Panpatte, D.G.; Jhala, Y.K.; Shelat, H.N.; Vyas, R.V. *Pseudomonas Fluorescens: A Promising Biocontrol Agent and PGPR for Sustainable Agriculture*. In *Microbial Inoculants in Sustainable Agricultural Productivity*; Springer India: New Delhi, India, 2016; pp. 257–270.

Disclaimer/Publisher's Note: The statements, opinions and data contained in all publications are solely those of the individual author(s) and contributor(s) and not of MDPI and/or the editor(s). MDPI and/or the editor(s) disclaim responsibility for any injury to people or property resulting from any ideas, methods, instructions or products referred to in the content.